New Ethyl Cellulose/Acrylic Hybrid Latexes and Coatings via Miniemulsion Polymerization

R. Chen, F. Chu, C. Gauthier, Laurent Chazeau, I. Chaduc, E. Bourgeat-Lami, M. Lansalot

Journal of Polymer Science Part A: Polymer Chemistry

New ethyl cellulose/acrylic hybrid latexes and coatings via miniemulsion polymerization

Journal:	*J. Polym Sci. Part A: Polym. Chem.*
Manuscript ID:	Draft
Wiley - Manuscript type:	Original Article
Keywords:	Ethyl cellulose, Acrylic, Miniemulsion polymerization < E, Hybrid latex, incompatibility < I, films < F

New ethyl cellulose/acrylic hybrid latexes and coatings via miniemulsion polymerization

R. Chen,[1, 2] F. Chu,[2] C. Gauthier, [3] L. Chazeau,[3] I. Chaduc,[1] E. Bourgeat-Lami,[1*] M. Lansalot[1*]

[1] Université de Lyon, Univ. Lyon 1, CPE Lyon, CNRS UMR 5265, Laboratoire de Chimie, Catalyse, Polymères et Procédés (C2P2), LCPP group, 43 Bd. du 11 Novembre 1918, F-69616, Villeurbanne, France.
[2] Institute of Chemical Industry of Forest Products, Chinese Academy of Forestry, 16 Suo Jin Wucun, 210042 Nanjing, China
[3] MATEIS, INSA-Lyon, 7 avenue Jean Capelle 69621 Villeurbanne Cedex, France

Abstract

Ethyl cellulose (EC) was incorporated into copolymer latexes via miniemulsion polymerization. The effects of EC viscosity and EC content on droplet size, particle size and polymerization kinetics were investigated. The higher the EC content and viscosity, the larger the droplet size and the less stable the latex suspension. Small droplets that could be efficiently nucleated were formed for the lower-viscosity EC but the latex still showed limited colloidal stability. This was attributed to some phase-incompatibility between EC and the acrylic polymer. These stability issues were overcome by using an oil-soluble initiator and a cross-linker. The later enabled to physically entrap EC inside the polymer particles while the former allowed *in situ* grafting of the growing acrylic radicals to the EC backbone decreasing thereby the extent of phase separation. Thermal-mechanical analyses evidenced that the films obtained from the hybrid latexes displayed better properties than the EC-free latex films or the physical blends. This supports the hypothesis of formation of hybrid latexes that synergistically combine the properties of the acrylic matrix and the EC polymer. Interestingly, a significant increase of the elastic modulus was observed between 50-90°C. This mechanical reinforcement was tentatively attributed to the formation of a percolating EC-based hybrid phase.

* Corresponding authors : lansalot@lcpp.cpe.fr and bourgeat@lcpp.cpe.fr

Keywords: ethyl cellulose, acrylic, miniemulsion polymerization, hybrid latex, incompatibility, films

1. Introduction

Cellulose is an abundant natural polymer with renewable and biodegradable characteristics.[1] It is widely used as an additive in membranes, pharmaceuticals and foodstuffs. Among cellulosic materials, ethyl cellulose (EC) is a chemically modified cellulose derivative which has attracted a particular attention in recent years. This material is used in a lot of fields such as plastics, coatings, rubbers, printing inks and insulated materials owing to its high dielectric strength and stability with light, heat, oxygen, damp, base and dilute acid. In addition, EC is highly compatible with phenolic resins, alkyds and plasticizers. It also shows a low residue on ignition after burning, can contribute to film toughness without any additives and can keep flexibility under low temperature. At last, EC films and plastics have exceptional mechanical strength and flexibility in a wide range of temperatures.[1] The cellulose backbone of EC can be readily chemically modified with synthetic polymers via different polymerization techniques, such as irradiation with ultraviolet light,[2] ring-opening polymerization[3] or atom transfer radical polymerization.[4-7] As typical examples, we can mention the synthesis of EC-graft-poly(ε-caprolactone) and their block copolymers with poly(L-lactide),[3] EC-graft-poly(ethylene glycol) allenyl methyl ether macromonomer[8] and EC-based amphiphilic copolymers with poly(acrylic acid) or poly(poly(ethylene glycol) methyl ether methacrylate pendant chains. In the field of emulsions, ethyl cellulose can be used as an emulsifier,[9] incorporated into coatings[10-11] or used to elaborate microspheres notably for drug delivery applications.[12-14] The most developed procedure for the preparation of EC pseudo-latexes relies on either the emulsification/solvent evaporation (ESE) process [15-16] (which consists in the dissolution of EC in a suitable solvent, its subsequent emulsification into water phase containing suitable emulsifying agent, and finally the solvent evaporation) or miniemulsification.[17] A process based on nanoprecipitation has also been reported.[18] Recently, Arias *et al.* synthesized core-shell particles consisting of a magnetic carbonyl iron core and a biocompatible ethyl cellulose shell using the ESE process.[19]

Although various cellulosic derivatives have been used for the elaboration of advanced materials for coating applications,[10, 20-21] to our knowledge, there is no work reporting the

incorporation of ethyl cellulose into polymer latex particles. In the present paper, EC was incorporated into polyacrylic latexes via miniemulsion polymerization with the ultimate goal of improving the properties of the resulting polymer film materials. Instead of physically blending EC and the latex suspension, we dispersed ethyl cellulose into acrylic monomers, formed nanosize droplets by sonication and then polymerized the EC-containing nanodroplets via miniemulsion polymerization. This method should not only enable achieving intimate mixing between EC and the acrylics but may also offer the opportunity to covalently link the EC to the polymer matrix. This work aimed at finding appropriate conditions to synthesize such latexes that should be colloidally stable and contain as much EC as possible. The mechanical properties of the films obtained from the hybrid latexes were compared to those of pure acrylic films.

2. Experimental Section

Materials.

Butyl acrylate (BA, 99+%, Aldrich), methyl methacrylate (MMA, 99%, Aldrich), triethylene glycol dimethacrylate (TEGDMA, 95%, Aldrich), hexadecane (HD, 99%, Acros Organics), ammonium persulfate (APS, 98%, Acros Organics), dilauroyl peroxide (LPO, 99%, Acros Organics), sodium dodecyl sulfate (SDS, 99%, Acros Organics), ethyl cellulose (EC, Aldrich) with viscosities of 10 and 100 cP (viscosity in 5 wt% solution of 80/20 toluene/ethanol) hereafter referred to as EC10 and EC100, respectively, were used as received. Water was deionized before use (Purelab Classic UV, Elga LabWater).

Ethyl cellulose characterization.

Molar masses and molar mass distributions of the commercial EC samples were determined by size exclusion chromatography (SEC) using a modular system comprising a Waters 515 HPLC pump and an autosampler 717Plus (Waters). A pre-column (PLgel 5 µm) and three columns [two PLgel 5 µm Mixed C (300x7.5 mm^2) and one PLgel 5 µm 500 Å (300x

7.5mm^2)] thermostated at 30°C were used with THF as eluent at a flow rate of 1 mL.min^{-1}. Waters 410 refractometer was used for detection and molar masses were calculated on the basis of a calibration curve using narrow polydispersity polystyrene standards. The viscosity of EC-monomer solutions was measured using a RFS III rheometer (Rheometric Scientific). The measurements were performed on approximately 20 g of liquid at 25°C. The reported viscosity values were taken at the plateau.

Solution polymerization.

Polymerizations in solution were performed in a three necked round-bottom flask equipped with a condenser, a thermometer, a magnetic stirrer and an argon inlet. The reaction vessel was loaded with a mixture of monomers (MMA/BA 50/50 by weight), EC (10 wt%/monomers) and toluene (targeted solid content=33wt%) and immersed in an oil bath. The mixture was degassed under argon for 30 minutes at room temperature while the temperature was raised to75°C. Finally, the introduction of LPO dissolved in toluene gave the zero time of the polymerization. Monomer consumption was followed by gravimetric analysis of samples withdrawn from the polymerization medium at different times. Molar masses and molar mass distributions of the dried polymers were calculated on the basis of a calibration curve using low polydispersity poly(methyl methacrylate) standards.

Latex synthesis and characterization.

Batch miniemulsion copolymerizations were performed in a glass-jacketed reactor equipped with a condenser and a nitrogen inlet. The monomers (BA and MMA, 50/50 by weight) were first mixed with the hydrophobe (HD), EC (if used) and the cross-linker (TEGDMA, if used). This organic phase was then added to the aqueous solution containing the surfactant (SDS) under vigorous stirring. The resulting mixture was then ultrasonicated (750W Vibracell 75042, amplitude 90%) for 5 minutes. The obtained miniemulsion was next introduced into the reactor and deoxygenated by purging with nitrogen for 20 min while the temperature was raised to 75°C. Finally, the addition of initiator (APS) gave the zero time of the polymerization. A slightly different procedure was followed when using an oil-soluble

initiator. LPO was dispersed into the organic phase before the sonication step and the polymerization was performed at 80°C. The experimental conditions of all the polymerizations performed in this study are displayed in Table 1 and Table 2.

Insert Tables 1 and 2 here

Monomer consumption was followed by gravimetric analysis of samples withdrawn from the polymerization medium at different times. The droplet and particle sizes (hydrodynamic diameter – D_d and D_p, respectively) were measured by dynamic light scattering (Zetasizer HS1000 from Malvern Instruments), and the data were collected using the fully automatic mode of the Zetasizer system. The mean size distribution, *Poly,* is a dimensionless measure of the distribution broadness determined from the autocorrelation function using a second-order method of cumulant analysis.[22] For a monodisperse sample, the poly value should theoretically be zero. In practice, a poly value for a "monodisperse" latex lies between 0 and 0.05. The poly value can be considered to have lost its significance for values above 0.15, but below a value of 0.5 useful comparisons between samples can be made. The number of droplets, Nd, or particles, Np (mL^{-1}_{Latex}), was calculated using the diameter obtained from DLS (either D_d or D_p, nm) according to equation (1), with τ the solid content of the dispersed phase (comprising the monomer and polymer present for a given conversion and expressed in $g.mL^{-1}_{Latex}$), and ρ ($g.cm^{-3}$) the density of the particles (taking into account the conversion).

$$\text{Np, Nd} = \frac{6\tau}{\rho\pi\,(\text{diameter})^3} \times 10^{21} \qquad (1)$$

Conductivity measurements were performed on a CDM83 conductimeter. A concentrated SDS solution (40 $g.L^{-1}$) was added drop wise to a known volume of water in the presence of APS and the conductivity of the solution monitored. The Critical Micelle Concentration (CMC) was determined to be 2.36 $g.L^{-1}$, in good agreement with values reported in the literature.[23] The evolution of conductivity versus SDS concentration below the CMC could be expressed as follows: Conductivity ($mS.cm^{-1}$) = 0.44×[SDS] ($g.L^{-1}$) + 0.0468. This allowed us to

determine the concentration of SDS in the aqueous phase for the miniemulsions.

Imaging techniques.

Transmission Electron Microscopy (TEM) analyses were carried out at the Centre Technologique des Microstructures (CTμ), Claude Bernard University, Villeurbanne, France. A drop of the diluted latex suspension was deposited on a formvar-coated copper grid and allowed to evaporate before observation at the accelerating voltage of 80 kV using a Philips CM120 microscope.

Film formation and film characterizations.

The film formation was carried out as follows. The desired amount of latex (10 g with 30% solid content) was first cast into a Teflon mould (8 cm in diameter) and then dried in an oven thermostated at 35°C overnight. The film was taken out of the pan, quickly washed with distilled water to get rid of the exuded emulsifier, and dried again at 35°C for 30 minutes.

The hybrid films were analyzed by Differential Scanning Calorimetry (DSC). Appropriate amounts of samples were sealed in aluminum pans. DSC thermo-scans of the materials were then recorded under a dry nitrogen atmosphere at a heating rate of 10°C.min^{-1} from 20 to 130°C, in two scans using a Setaram DSC 131 apparatus.

Dynamic Mechanical Analysis (DMA) measurements were performed on rectangular specimens (15 x 6 x 2 mm^3) with an inverted torsion pendulum apparatus already described in literature.[24] This device works in a helium atmosphere, in the temperature range of 100-700K and frequency range of 5.10^{-5} Hz to 5 Hz. The storage (G') and loss (G'') parts of the dynamic shear modulus, and so the internal friction tanδ (G''/G') were measured as a function of temperature (from 173 to 373 K), with a heating rate of 1°/min, and a frequency of 0.1 Hz.

3. Results and Discussion

3.1. Characteristics of the EC powders and of the resulting monomer solutions

Of central importance for the use of ethyl cellulose in miniemulsion polymerization are its physicochemical properties, and notably the molar mass, the ethoxyl content and the glass transition temperature (Tg). Table 3 summarizes the experimental values determined for the two different EC grades employed in this work. It is seen that EC10 and EC100 have the same ethoxyl content and similar Tgs but different molar masses in agreement with the viscosity data.

Insert Table 3 here

Since the viscosity of the monomer phase is a key factor for a successful emulsification, we investigated the effect of EC content on the viscosity of the monomer solution. To do so, increasing amounts of EC were dissolved into a 50/50 (wt/wt) MMA/BA mixture and the viscosity of the resulting solutions was determined as detailed in the experimental part. The results are reported in Table 4. As expected, the values measured for 5wt% of both types of EC were in good agreement with the supplier data and increased with increasing EC content.

Insert Table 4 here

3.2. Preparation of EC-loaded miniemulsion droplets

As reported in literature, the viscosity of the dispersed phase influences the droplet size of oil-in-water emulsions.[25-27] Figure 1 shows the evolution of the MMA/BA droplet size as a function of sonication time for different amounts of EC100. As expected, the droplet size decreased with increasing sonication time and increased with increasing EC content that is to say with increasing the viscosity of the EC-acrylate solution. For EC contents comprised between 5 and 15wt%, the droplets were stable. However, for higher EC contents, we could not produce stable miniemulsion droplets even when increasing the applied power/volume

ratio. Mabille *et al*. proposed a relationship between the droplet size, D_d, and the viscosity ratio, R, between the dispersed and continuous phase.[28] For stable miniemulsions (0 to 15 wt% of EC), the evolution of the droplet diameter with the viscosity ratio could be fitted with a power law which agrees well with that of Mabille *et al*.: $D_d = 49 \times R^{0.21}$.

Insert Figure 1 here

3.3. Synthesis of EC-based hybrid latexes through miniemulsion polymerization

Effect of EC content and EC viscosity on droplet nucleation and latex stability

In a first series of experiments, we studied the effect of EC100 on droplet nucleation and latex particle formation keeping in mind the high viscosity of the dispersed phase for high EC100 contents. Table 2 reports the final monomer conversion for each experiment while Figure 2 displays the evolution of particle size with conversion. In the absence of EC or for a low amount of EC (typically 5wt%), the system shows the expected features of miniemulsion polymerization that is to say a constant evolution of particle diameter with conversion indicating efficient droplet nucleation. However, when increasing the EC100 content to 10 and 15wt%, the particle diameter decreased with increasing conversion while the monomer conversion levelled off. In addition, some coagulum, the amount of which was not quantified at this stage, was formed in both cases. Note that some coagulum was also observed for 5wt% of EC but in lower proportions.

Insert Figure 2 here

These results can be interpreted as follows. The interfacial area developed by the large droplets formed in the presence of a high amount of EC is too low to ensure efficient capture of the growing oligoradicals. Given the relatively high solubility of MMA in water (15 $g.L^{-1}$), homogeneous nucleation is thus likely to occur, giving rise to the formation of small particles

stabilized by surfactant. As the monomer diffuses from the large droplets to these secondary-nucleated particles, EC would be expelled out of the original miniemulsion droplets as it cannot transport through the water phase. This would result in latex coagulation as there would not be enough surfactant to stabilize both the newly created particles and the EC polymer. As a direct consequence, the formation of coagulum leads to underestimated monomer conversions. The higher the EC content, the less stable the latex suspension and, thus the lower the monomer conversion at the plateau.

As mentioned above, the large droplet size is due to the high viscosity of the dispersed phase. Therefore, in an attempt to decrease the droplet size while maintaining reasonable EC contents, the lower viscosity EC grade (i.e. EC10) was evaluated under otherwise identical experimental conditions. In this new series of experiments, the amount of coagulum (expressed in weight fraction of the total amount of solid produced during the polymerization) was determined experimentally by weighing the solid residue. Although the use of EC10, that has a lower viscosity than EC100, gave rise to lower droplet sizes (see Run 5 in Table 2), the resulting latex still contained some amount of coagulum. In this case (Figure 3), the particle size first increased to 250 nm and then decreased to values lower than the size of the parent miniemulsion while concurrently, the monomer conversion levelled up to around 70%. In addition, it is worth noting that the transitory increase in size was concomitantly accompanied with a decrease in polymerization rate.

Insert Figure 3 here

The increase in particle size at low conversion indicates that the droplets were unstable and coalesced during the early stages of polymerization. Different reasons may explain why the droplets were not stable in the presence of EC10. First, EC and the polymer matrix may be not compatible with each other, thus inducing phase separation. Indeed, EC solubility inside the particles would decrease as the polymerization proceeds ultimately leading to phase separation and droplet coalescence. In addition, EC is known to be able to reduce the interfacial tension of water-in-oil emulsion.[29] EC is therefore expected to be more compatible

with the water phase than with the polymer. EC migration at the oil/water interface may emphasize the phase separation process. Therefore, as before for EC100, EC10 is likely to be excluded from the latex particles upon polymerization. This last hypothesis was supported by TEM observation of the hybrid latex after polymerization which clearly shows the presence of free EC displaying an elongating rod-like shape, together with spherical EC-free latex particles (Figure 4b).

Insert Figure 4 here

To support the assumption of EC preferential location at the oil/water interface, we determined the amount of SDS present in the continuous phase for different systems (Table 5). Since most of the surfactant is adsorbed onto the surface of the droplets which exhibit a high interfacial area, the SDS concentration in the aqueous phase is expected to be lower than the CMC. This was confirmed by measuring the conductivity of the miniemulsions for the two grades of EC. Table 5 also shows that for a given EC grade, the amount of free SDS increases with increasing EC content in agreement with the increase in droplet size. In addition, for the same initial amount of EC, the droplet size is significantly lower in the case of EC10, while at the same time, the concentration of SDS in the aqueous phase is higher. This suggests that EC10 is preferentially located at the interface of the monomer droplets with water, thus displacing part of the SDS molecules. Despite the fact that EC100 has higher viscosity and molar mass, and probably less affinity for the water phase than EC10, the above scenario also holds for this EC grade and may account for the poor latex stability also observed in this case.

Insert Table 5 here

Addition of a cross-linker

It is well-known that the use of a cross-linker leads to the formation of a polymer network of limited mobility which might decrease the extent of phase separation.[30] To prevent any

transfer of ethyl cellulose to the aqueous phase and to physically hold EC inside the particles, the next series of experiments was thus performed with triethylene glycol dimethacrylate (TEGDMA) as a cross-linking agent using 4.7 wt% of TEGDMA with respect to the monomers/EC mixture (run 6, Table 2). The amount of coagulum was effectively lowered but was still too high to be acceptable (26 wt% *vs* 38 wt% without TEGDMA). In addition, the evolution of particle size with conversion followed almost the same trend with or without TEGDMA (i.e. the particle size first increased and then decreased). In conclusion, the sole use of TEGDMA was not able to prevent EC diffusion and improve latex stability.

Another effective means of keeping EC inside the particles and decrease the extent of phase separation would be to chemically graft EC to the polymer chains constituting the particles. Indeed, many studies report in the literature the formation of graft copolymers from the backbone of cellulose and cellulosic derivatives using radical initiators.[31-35] APS being located in the water phase, the formation of radicals on the EC backbone may not be efficient. This is why the nest series of experiment was performed with an organo-soluble initiator, the dilauroyl peroxide (LPO). Effectively, when LPO was used as initiator and TEGDMA as cross-linker, the obtained latex (run 7) was perfectly stable (no coagulum) with 100% conversion. LPO being closely located to EC, it is thus very likely that EC was implicated in the free radical process to form graft copolymers. Note that in this case, particle size increases with increasing conversion indicating the occurrence of some limited-coalescence. In other words, we have created fewer particles than the number of monomer droplets initially present in the reactor. A similar discrepancy between the initial number of droplets and the final number of latex particles has already been reported in the literature for miniemulsion polymerizations performed in the presence of oil-soluble initiators.[36-37]

Insert Figure 5 here

What is worth to be noted is the particular morphology of the particles (Figure 6a) even in the absence of EC (run 8, Figure 6b). Indeed, the majority of the particles (which are polydisperse in size) seem to be constituted of two phases with different electron densities (one dense, the other not) leading to a half moon-like morphology. This morphology is likely due to an

interplay of thermodynamic and kinetic factors operating during the polymerization process. Indeed, the reactivity ratios for MMA/BA copolymerization (r_{MMA} = 2.55 ± 0.35 ; r_{BA} = 0.36 ± 0.08 [38]) indicate that MMA is more reactive than BA and thus preferentially incorporated leading to a compositional drift. In addition, the presence of the cross-linker TEGDMA whose reactivity is likely similar to that of MMA, will lead to the formation of a PMMA-rich and cross-linked phase. Due to the limited swelling of this phase by the monomer(s), polymerization will eventually lead to asymmetrical particles with a PBA-rich phase (with a low electron density) according to mechanisms likely similar to those depicted by Sheu *et al.*[39] and Mock *et al.*[40] In these works, it was reported that heating monomer-swollen cross-linked polymer seed caused the phase separation of the monomer from the seed in the form of a non-uniform bulge, which upon polymerization resulted into the formation of asymmetrical particles. Taking these considerations into account, it though remains quite difficult to predict which phase (PMMA or PBA) would be enriched in EC. What could be drawn from TEM observations was that free EC was not detectable on any TEM images (Figure 6b). This, together with the absence of coagulum, would indicate an efficient encapsulation of EC inside the particles. The fact that EC crystals could not be distinguished could be explained by the reactivity of radical initiators towards cellulose and its derivative. Indeed, the use of oxygen-centered radicals has been reported to strongly degrade cellulosic backbone. The addition of a radical initiator such as LPO could effectively lead to the formation of EC-based graft copolymers in the presence of vinyl monomer as shown in Scheme 1.

To support this assumption, copolymerization of MMA/BA was carried out in toluene (67wt% of solvent) without or with EC (10wt% of EC10). The polymerization performed in the presence of EC resulted in a lower molar mass providing further evidence of EC implication in the free radical process. Indeed, the molar mass was unchanged when EC was simply blended with the copolymer.

Insert Figure 6 here

Insert Scheme 1 here

The combined use of TEGDMA and LPO giving satisfactory results in terms of both colloidal stability and monomer conversion, the EC10 content was then increased from 10 to 15 wt% (Run 9, data not shown). The reaction behaved in a very similar way at the beginning of the polymerization but the latex then became unstable. Increasing the amount of TEGDMA for a fixed amount of EC (8.4 and 17 wt%, for runs 10 and 11, respectively) did not improve the latex colloidal stability. Moreover, the higher the amount of TEGDMA, the lower was the final conversion. This could be due to the high cross-linking density of the latex particles which might limit their swelling capacity by the monomer.

The conditions described above (LPO, 10 wt% EC, and 4.7 wt% TEGDMA) were then applied to EC100 grade (run 12). Similarly to the APS-initiated system, the droplet size is higher when the viscosity of EC is increased. Despite the presence of TEGDMA, the obtained latex was not stable and 13 wt% of coagulum was obtained which can account for the limiting conversion observed in this case (Figure 7). As seen in Figure 8, the particle size distribution is larger than for the EC10-based latex in agreement with DLS measurement (Table 1) while the particles exhibit a similar half-moon morphology.

Insert Figure 7 here

Insert Figure 8 here

As evidenced by all the results discussed above, the synthesis of colloidally stable latexes incorporating a high amount of EC is not straightforward. We however succeeded in the formation of stable acrylic latexes incorporating up to 10wt% of low viscosity EC10. The film properties of these latexes have then been studied and compared to those of physical blends containing the same amount of EC. The results are presented below.

3.4. Thermomechanical properties of EC-based hybrid latexes

This section will focus on the latex obtained in the presence of TEGDMA, LPO and 10wt% of

EC 10 (run 7). The properties of the films obtained from this latex will be compared to those of EC alone, of the film formed from an EC-free latex (run 8, referred to as the blank matrix) and/or of a physical blend obtained by mixing 10 wt% of EC10 with the blank matrix.

Differential scanning calorimetry

The film formed from the hybrid latex (run 7), the blank matrix and the physical blend were first characterized using DSC. The blank matrix shows only one Tg at 17.5°C. No clear shift of the Tg value was noticed for the physical blend (Tg around 17°C). In contrast, for the hybrid latex, a 3 °C shift towards lower temperature was observed. This result supports the assumption of latex hybridization and chemical incorporation of EC polymers by free radical polymerization as represented in Scheme 1.

Thermal gravimetric analysis

TGA experiments were then performed on EC and the different films (Figure 9). For ethyl cellulose, the obtained curve is in agreement with the literature.[41] The thermal degradation of the acrylic polymer starts at around 190 °C and is almost complete at 450°C (run 8). Given the low weight fraction of EC10, the curve corresponding to the physical blend is very close to that of the acrylic polymer with a degradation beginning at 181°C. It is worth noting that this curve corresponds to the weighted summation of the EC10 curve and of the EC-free latex curve. In contrast, the degradation is significantly delayed in the case of the hybrid latex (run 7: 218°C) indicating that EC provides improved thermal resistance to the hybrid film.

Insert Figure 9 here

Dynamic mechanical analysis

DMA experiments were performed on the different films to characterize the influence of EC on their viscoelastic properties. Figure 10 presents the comparison between the films obtained from the EC-free latex, the physical blend and the EC10-based hybrid latex.

Insert Figure 10 here

DMA curve of the physical blend incorporating 10wt% of EC is very similar to that of the blank matrix. The main relaxation, indicated by a large modulus drop and a tanδ peak, occurs at the same temperature for both materials; the loss factor peak is located at T = 42°C. This confirms the DSC results which suggested that the mixing of the matrix with 10wt% of EC10 does not modify the glass transition temperature. The addition of EC10 only slightly increases the modulus value. This increase vanishes at temperature above 90°C, i.e. when the temperature approaches that of the glass transition temperature of EC10. For the hybrid material, the G' decrease associated with Tα starts earlier, observation which is also in agreement with the DSC measurements. Furthermore, in that case, a second peak is observed at temperature around 107°C. These results can be associated with the composition drift discussed above. The main relaxation shift toward lower temperature would be due to a polymer phase poorer in MMA units. Within this assumption, the second peak, at temperature around 107°C, could be attributed to a PMMA enriched phase, since it is well known that the PMMA phase has a relaxation temperature in this temperature region. However, if the peak at 107°C is due to a composition drift of the copolymer; it should also be present in the DMA curve of the EC-free latex which is not the case. One could also argue that the peak at 107°C is due to the EC α relaxation. Indeed, this one has clearly been observed at this temperature in EC/acrylic blends when the EC contents are above 30% (DMA results not presented here). However, in the present case, the EC content is much lower than 30% (i.e., 10wt%) and the peak is actually located at temperature slightly lower than the EC relaxation temperature which is around 120°C. At last, it must be noted that the presence of EC in the hybrid leads to a large increase of the modulus at temperature between 30°C and 100°C. Such an increase of the modulus by a factor 10 is too high to be attributed to the reinforcement by isolated EC domains. Moreover, no EC domains could be identified in the TEM picture of the hybrid latex (Figure 6b) while there is no significant reinforcement of the modulus in the glass transition region (prior to the main relaxation). Thus, it can be proposed that the EC10 molecules have been intimately linked to the polymer chains, giving birth to a second phase with a glass transition temperature slightly above 100°C. Given the large modulus at temperature below

this Tg, this phase likely percolated, creating a network rigid at temperature below its glass transition temperature.

Conclusions

A series of EC-containing hybrid latexes were prepared by reacting simultaneously ethyl cellulose, MMA and BA in miniemulsion polymerization. It was shown that the droplet size and latex stability were strongly dependent on EC viscosity and EC content. When APS was used as initiator, the higher the EC content and EC viscosity, the less stable were the latex suspensions. This was thought to be due to EC being expelled out of the latex particles upon polymerization because of phase incompatibility between EC and the acrylic polymer. Stable hybrid latexes free of any coagulum and containing up to 10wt% of low viscosity EC could be successfully obtained by using a cross-linker that physically retained EC inside the latex particles, and an oil-soluble initiator capable of undergoing chemical graft reactions with the cellulose backbone increasing thereby chemical compatibility. The films issued from the hybrid latex showed superior thermal and mechanical properties compared to the EC-free latex film and to the film made from a physical blend of EC and EC-free latex. It was proposed that *in-situ* grafting of acrylic radicals to EC led to the formation of an EC-based hybrid polymer phase that formed a rigid percolating network at temperatures below its glass transition temperature.

Acknowledgements: C. Graillat and P.Y. Dugas are acknowledged for their help in viscosity and conductimetry measurements.

References

1. a) Klemm, D.; Philipp, B.; Heinze, T.; Heinze, U.; Wagenknecht, W. Comprehensive Cellulose Chemistry. Vol. 2, Wiley-VCH, Weinheim, pp 220 (1998) ; b) Klemm, D.;

Heublein, B.; Fink, H.P.; Bohn. A. Angew. Chem. Int. Ed. 2005, 44, 3358-3393.

2. Abdel-Razik, E.A. J. Photochem. Photobiol. A: Chem. 1993, 73, 53-58.
3. Yuan, W.; Yuan, J.; Zhang, F.; Xie, X. Biomacromolecules 2007, 8, 1101-1108.
4. Tang, X.D.; Gao, L.C.; Fan, X.H.; Zhou, Q.F. J. Polym. Sci., Part A: Polym. Chem. 2007, 45, 1653-1660.
5. Shen, D.W.; Yu, H.; Huang. Y. J. Polym. Sci., Part A: Polym. Chem. 2005, 43, 4099-4108.
6. Li, Y.; Liu, R.; Liu, W.; Kang, H.; Wu, M.; Huang, Y. J. Polym. Sci., Part A: Polym. Chem. 2008, 46, 6907-6915.
7. Kang, H.L.; Liu, W.Y.; He, B.Q.; Shen, D.W.; Ma, L.; Huang, Y. Polymer 2006, 47, 7927-7934.
8. Aggour, Y.A. J. Mater. Sci. 2000, 35, 1623-1627.
9. Lim, D.W.; Song, K.G.; Yoon, K.J.; Ko, S.W. Eur. Polym. J.l 2002, 38, 579–586.
10. Hutchings, D.; Clarson, S.; Sakr, A. Int. J. Pharm. 1994, 104, 203-213.
11. Wennerstrand Wallstroem, A.; Olsson, M.; Jaernstroem, L.; Koschella, A.; Fenn, D.; Heinze, T. J. Colloid Interf. Sci. 2008, 327, 51-57
12. Yang, C.Y.; Tsay, S.Y.; Tsiang, R.C.C. J. Microencapsulation 2001, 18, 223-236.
13. Choudhury, P. K.; Kar, M. J. Microencapsulation 2009, 26, 46-53.
14. Palmieri, G.F.; Grifantini, R.; Di Martino, P.; Martelli, S. Drug Dev. Ind. Pharm. 2000, 26, 1151-1158.
15. Gallardo, V.; Morales, M.E.; Ruiz, M.A.; Delgado, A.V. Eur. J. Pharm. Sci. 2005, 26, 170-175.
16. Gallardo, V.; Morales, M.E.; López-Viota, J.; Durán, J.D.G.; Ruiz. M.A. J. Appl. Polym. Sci. 2006, 102, 847–851.
17. Vanderhoff, J.W., El-Aasser, M.S., Ugelstad, J. 1979. U.S. Patent No. 4,177,177, USA.
18. Thioune, O.; Briançon, S.; Devissaguet, J.P.; Fessi, H. Drug Dev. Res. 2000, 50, 157-162.
19. Arias, J.L.; López-Viota, M.; Ruiz, M.A.; López-Viota, J.; Delgado, A.V. Int. J. Pharm. 2007, 339, 237-245.

20. Annable, T.; Gray, I.; Lovell, P.A.; Richards, S.N.; Satgurnathan, G.. Progr. Colloid Polym. Sci. 2004, 124, 159-163.
21. Janssen, B. J. W.; Kroon, G.; Kruythoff, D.; Salomons, W. G.. 1996. WO Patent No 014357.
22. a) Koppel, D.E. J. Chem. Phys. 1972, 57, 4814-4820. b) International Standard ISO 13321. Methods for determination of particle size distribution. Part 8: Photon Correlation Spectroscopy, International Organization for Standardization (ISO) 1996.
23. Erdem, B.; Sully, Y.; Sudol, E. D.; Dimonie, V.; El-Aasser, M. S. Langmuir 2000, 16, 4890-4895.
24. Etienne, S.; Cavaille, J.Y.; Perez, J.; Point, R.; Salvia, M. Rev. Scientific Instruments 1982, 53, 1261-1266.
25. Blythe, P. J.; Morrison, B. R.; Mathauer, K. A.; Sudol, E. D.; El-Aasser, M. S. Langmuir 2000, 16, 898-904.
26. do Amaral, M.; Bogner, A.; Gauthier, C.; Thollet, G.; Jouneau, P-H.; Cavaille, J.Y.; Asua, J.M. Macromol. Rapid Commun. 2005, 26, 365-368.
27. Jahanzad, F.; Karatas, E.; Saha, B.; Brooks, B-W. Coll. Surf. A: Physicochem. Eng. Aspects 2007, 302, 424-429.
28. Mabille, C.; Leal-Calderon, F.; Bibette, J.; Schmitt, V. Europhys. Lett. 2003, 61, 708-714.
29. Melzer, E.; Kreuter, J.; Daniels, R. Eur. J. Pharm. Biopharm. 2003, 56, 23-27.
30. Luo, Y.; Zhou, X. J. Polym. Sci., Part A: Polym. Chem. 2004, 42, 2145-2154.
31. Nishioka, N.; Kosai, K. Polym. J. 1981, 13, 1125-1133.
32. Nishioka, N.; Minami, K.; Kosai, K. Polym. J. 1983, 15, 591-596.
33. Abdel-Razik, E.A. Polymer 1990, 31, 1789-1744.
34. Aggour, Y.A. ; Abdel-Razik, E.A. Eur. Polym. J. 1999, 35, 2225-2228.
35. Wang, L.; Dong, W.; Xu, Y. Carbohydrate Polymers 2007, 68, 626-636.
36. Asua, J. M.; Rodriguez, V. S.; Sudol, E. D.; El Aasser, M. S. J. Polym. Sci., Polym. Chem. 1989, 27, 3569-3587.
37. Graillat, C.; Guyot, A. Macromolecules 2003, 36, 6371-6377.
38. Buback, M.; Feldermann, A.; Barner-Kowollik, C.; Lacík, I. Macromolecules 2001, 34,

5439-5448.

39. Sheu, H. R.; El-Aasser, M. S.; Vanderhoff, J. W. J. Polym. Sci., Part A: Polym. Chem. 1990, 28, 629-651.

40. Mock, E. B.; De Bruyn, H.; Hawkett, B. S.; Gilbert, R. G.; Zukoski, C. F. Langmuir 2006, 22, 4037-4043.

41. Chen, K. ; Lü, Z. ; Ai, N. ; Huang, X. ; Zhang, Y. ; Ge, X. ; Xin, X. ; Chen, X. ; Su, W. Solid State Ionics 2007, 177, 3455-3460.

TABLE CAPTIONS

Table 1. General Recipe for the Miniemulsion Polymerizations of Methyl Methacrylate (MMA)/Butyl Acrylate (BA) in the presence of Ethyl Cellulose (EC)

Table 2. Summary of experimental conditions of all the miniemulsion polymerizations performed in this study. Effects of synthetic parameters on droplet size, particle size, monomer conversion and weight fraction of coagulum.

Table 3. Physicochemical features of EC samples of increasing viscosities

Table 4. Viscosities of a series of EC-acrylate monomer solutions as a function of EC content and EC grade.

Table 5. Droplet size, conductivity and concentration of free SDS as a function of EC grade and EC content for EC-containing miniemulsions.

Table 1. General Recipe for the Miniemulsion Polymerizations of Methyl Methacrylate (MMA)/Butyl Acrylate (BA) in the presence of Ethyl Cellulose (EC)

Organic phase	
MMA/BA (50/50 by weight)	20% solid content
HD (wt%)[a]	6.7
EC (wt%)[a]	5-20
TEGDMA (wt%)[a]	4.7-17
LPO [b] (wt%)[a]	0.5
Water phase	
Deionized water	105 g
SDS (wt % [a])	1
APS [b] (wt % [a])	0.5

[a] With respect to monomers or monomers/EC mixture; [b] Polymerization temperature: 80°C with LPO, 75°C with APS.

Table 2. Summary of experimental conditions of all the miniemulsion polymerizations performed in this study. Effects of synthetic parameters on droplet size, particle size, monomer conversion and weight fraction of coagulum.

Run	EC type	MMA (g)	BA (g)	EC (g)	EC (wt%)[a]	Initiator	TEGDMA (g)	D_d (nm)	*Poly*	D_p (nm)	*Poly*	Conversion (%)[b]	Coagulum (wt%)[c]
1	/	22.5	22.5	0	0	APS	/	111	0.210	109	0.017	100	0
2	EC100	21.375	21.375	2.25	5	APS	/	139	0.149	119	0.039	89	ND[d]
3	EC100	20.25	20.25	4.5	10	APS	/	219	0.148	139	0.038	82	ND
4	EC100	19.125	19.125	6.75	15	APS	/	354	0.595	86	0.310	74	ND
5	EC10	20.25	20.25	4.5	10	APS	/	143	0.161	101	0.022	68	38
6	EC10	20.25	20.25	4.5	10	APS	2.1	148	0.149	120	0.056	85	26
7	EC10	20.25	20.25	4.5	10	LPO	2.1	105	0.181	180	0.064	100	0
8	/	22.5	22.5	0	0	LPO	2.1	141	0.194	230	0.064	56	0
9	EC10	19.125	19.125	6.75	15	LPO	2.1	148	0.173	205	0.121	55	12
10	EC10	19.125	19.125	6.75	15	LPO	3.8	157	0.142	219	0.056	62	10
11	EC10	19.125	19.125	6.75	15	LPO	7.65	156	0.142	214	0.072	24	21
12	EC100	20.25	20.25	4.5	10	LPO	2.1	199	0.127	280	0.109	71	13

[a] In wt% to monomers; [b] polymerization time = 90 min; [c] based on the total weight of polymer and EC; [d] ND = not determined

Table 3. Physicochemical features of EC samples of increasing viscosities

EC grade	EC10	EC100
Viscosity (cP) [a]	10	100
M_n (g.mol^{-1})	19 470	35 280
M_w (g.mol^{-1})	55 330	138 300
M_w/M_n	2.8	3.9
Ethoxyl content (%) [b]	48	49
Tg (°C)	122	128

[a] As determined by the supplier for a 5 wt% EC solution of 80/20 toluene/ethanol. [b] According to the provider, an ethoxyl content of 48% corresponds to a degree of substitution (D.S.) of Et functionalities on the cellulose backbone in the range of 2.25-2.58 mol ethyl per mol cellulose.

Table 4. Viscosities of a series of EC-acrylate monomer solutions as a function of EC content and EC grade.

EC grade		**EC10**			**EC100**	
EC content (%)	5	10	15	5	10	15
Viscosity of EC/ acrylate solution (cP)	10	100	410	120	1380	9370[a]

[a] This value should be considered with caution due to the high viscosity of the solution.

Table 5. Droplet size, conductivity and concentration of free SDS as a function of EC grade and EC content for EC-containing miniemulsions.

EC grade	EC content (%)	Droplet size (nm)	Conductivity (S/cm)	$[SDS]_{free}$ ($g.L^{-1}$) [a]
EC10	5	105	778	1.68
EC10	10	143	909	1.98
EC10	15	174	1031	2.26
EC100	5	145	735	1.58
EC100	10	225	864	1.87

[a] CMC value determined for SDS in an APS/water solution = 2.36 $g.L^{-1}$.

CAPTION TO THE FIGURES

Scheme 1. Mechanism for free-radical grafting and degradation of EC, adapted from the one proposed in reference 20.

Figure 1. Droplet diameter *vs* sonication time for EC100-containing acrylic miniemulsions. The lines are guides for the eye. See Table 2 for experimental details.

Figure 2. Evolution of particle size *vs* conversion during miniemulsion polymerization of MMA and BA in the presence of increasing EC100 contents. The lines are guides for the eye.

Figure 3. Evolution of monomer conversion and particle size during miniemulsion polymerization of MMA and BA in the presence of 10 wt% of EC10 (run 5) or EC100 (run 3). The lines are guides for the eye.

Figure 4. TEM pictures of EC10-containing a) miniemulsion and b) latex (EC content = 10 wt%, run 5). Note that for the miniemulsion, only ethyl cellulose is visible since the droplets disappear upon TEM observation.

Figure 5. Effect of the addition of a cross-linker on the evolution of monomer conversion and particle size during miniemulsion polymerization of MMA and BA initiated by APS or LPO in the presence of 10 wt% of EC10. The lines are guides for the eye.

Figure 6. TEM pictures of LPO/TEGDMA-based systems a) without EC (run 8) and b) with 10 wt% of EC 10 (run 7).

Figure 7. Evolution of monomer conversion and particle size during miniemulsion polymerizations of MMA and BA initiated by LPO in the presence of 4.7 wt% of TEGDMA and 10 wt% of EC10 (run 7) or EC100 (run 12). The lines are guides for the eye.

Figure 8. TEM image of EC100-based latex particles elaborated with LPO as initiator and TEGDMA as cross-linker (run 12).

Figure 9. TGA curves of EC10 powder, an EC-free latex (run 8), a physical blend of EC10 powder (10 wt%) and an EC-free latex (run 8), and EC10-based hybrid latex (10 wt%, run 7).

Figure 10. DMA curves of EC-free latex (run 8), of physical blend of latex and EC10 powder (10 wt%) and of EC10-based hybrid latex (10 wt%, run 7).

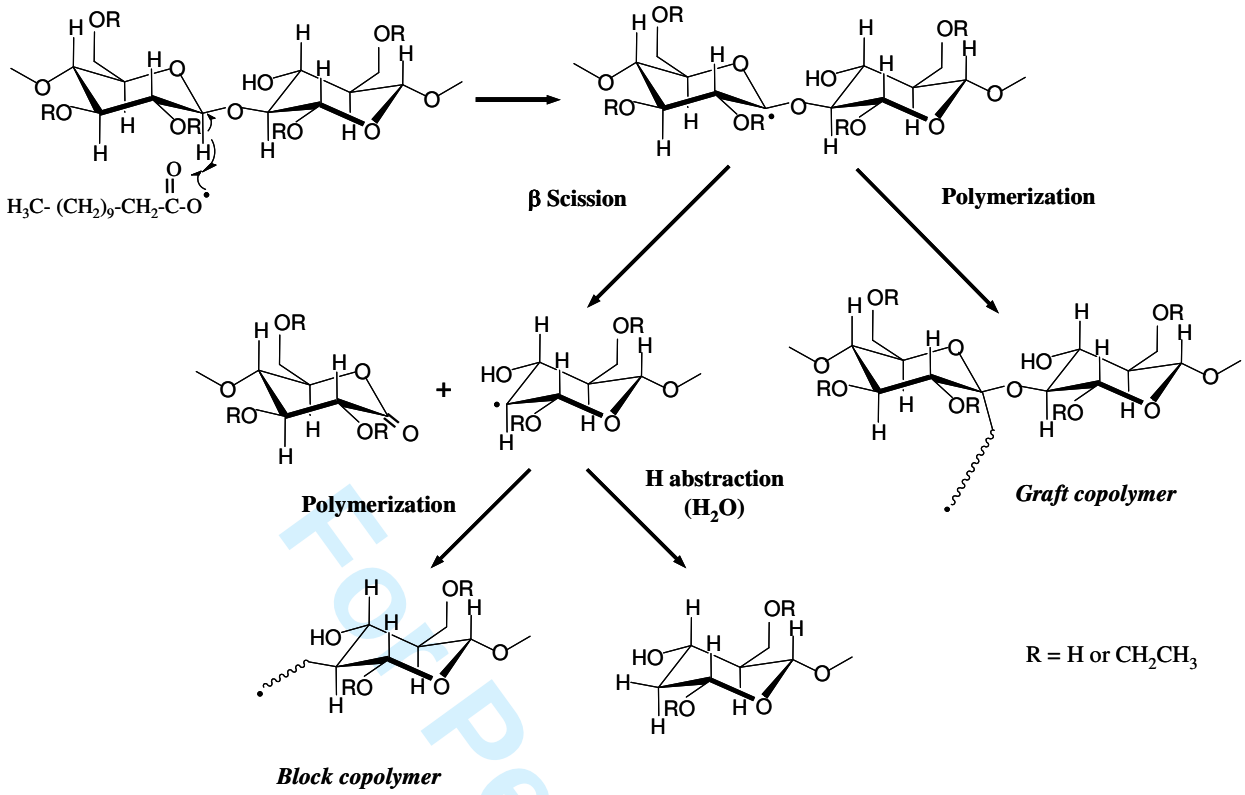

Scheme 1. Mechanism for free-radical grafting and degradation of EC, adapted from the one proposed in reference 20.

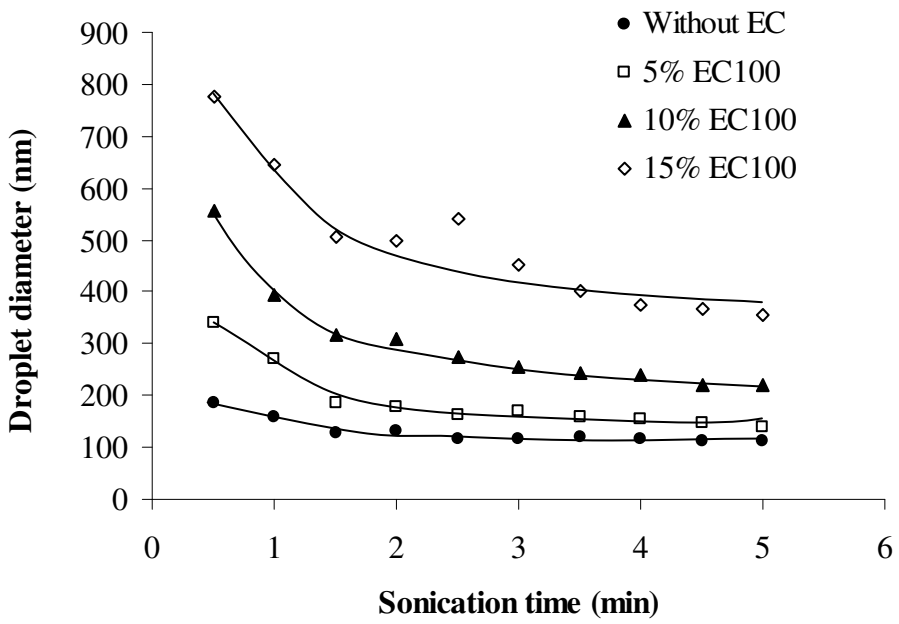

Figure 1. Droplet diameter *vs* sonication time for EC100-containing acrylic miniemulsions. The lines are guides for the eye. See Table 2 for experimental details.

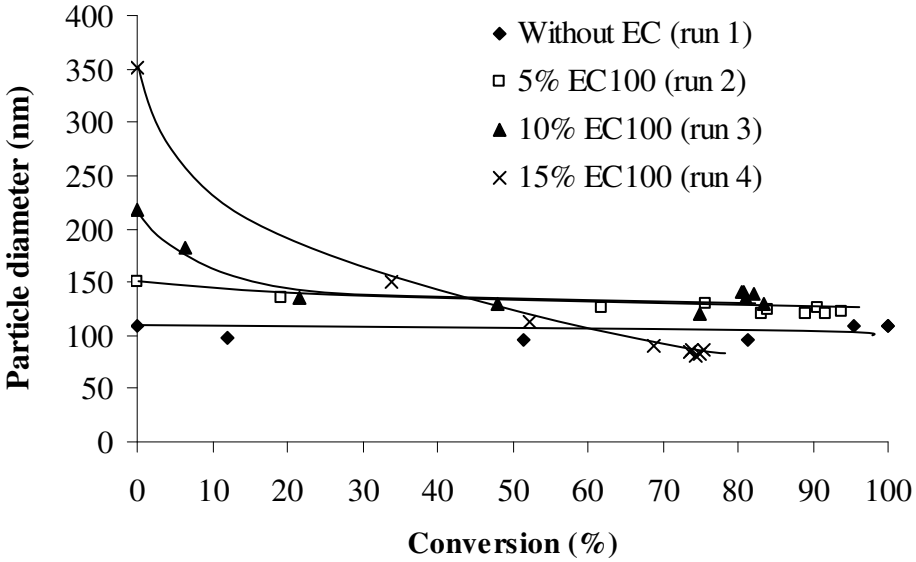

Figure 2. Evolution of particle size *vs* conversion during miniemulsion polymerization of MMA and BA in the presence of increasing EC100 contents. The lines are guides for the eye.

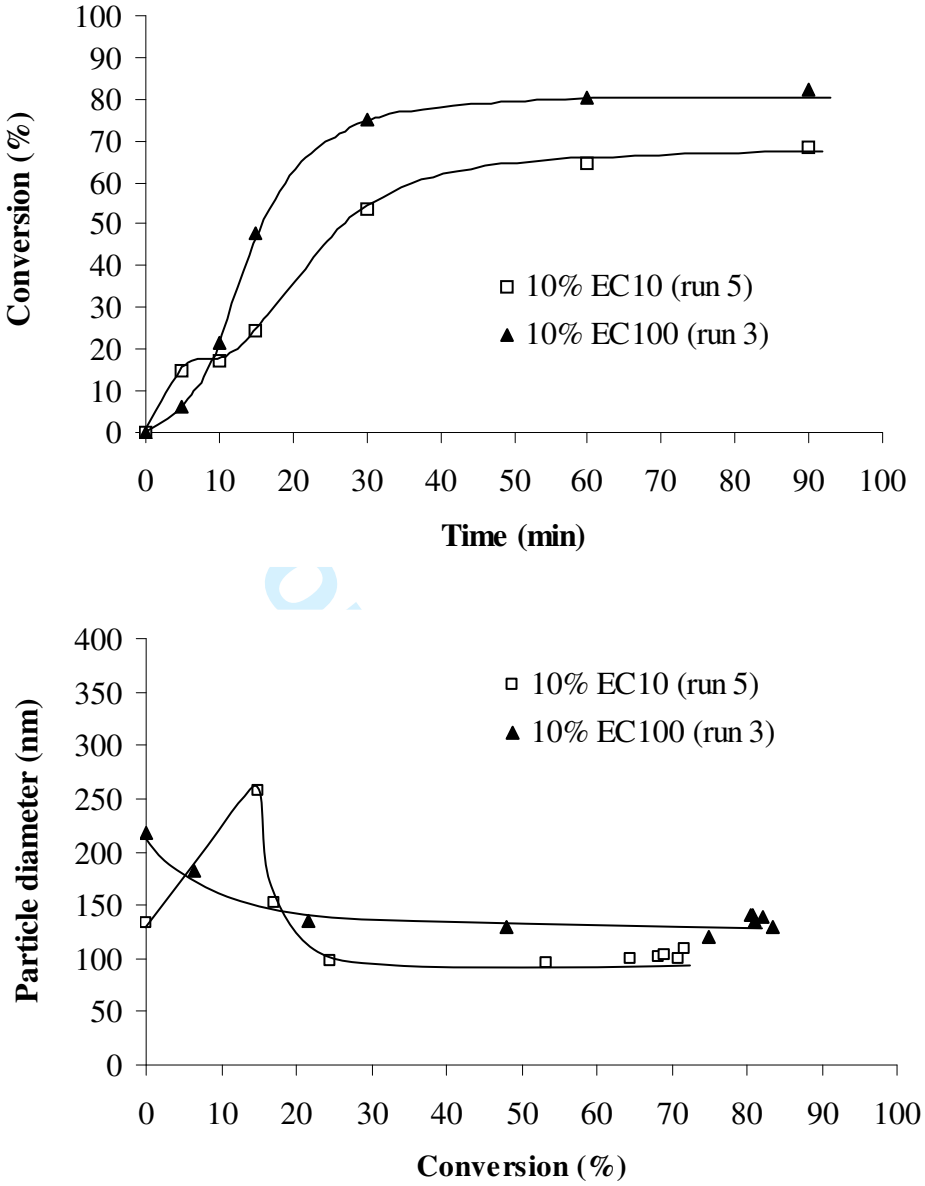

Figure 3. Evolution of monomer conversion and particle size during miniemulsion polymerization of MMA and BA in the presence of 10 wt% of EC10 (run 5) or EC100 (run 3). The lines are guides for the eye.

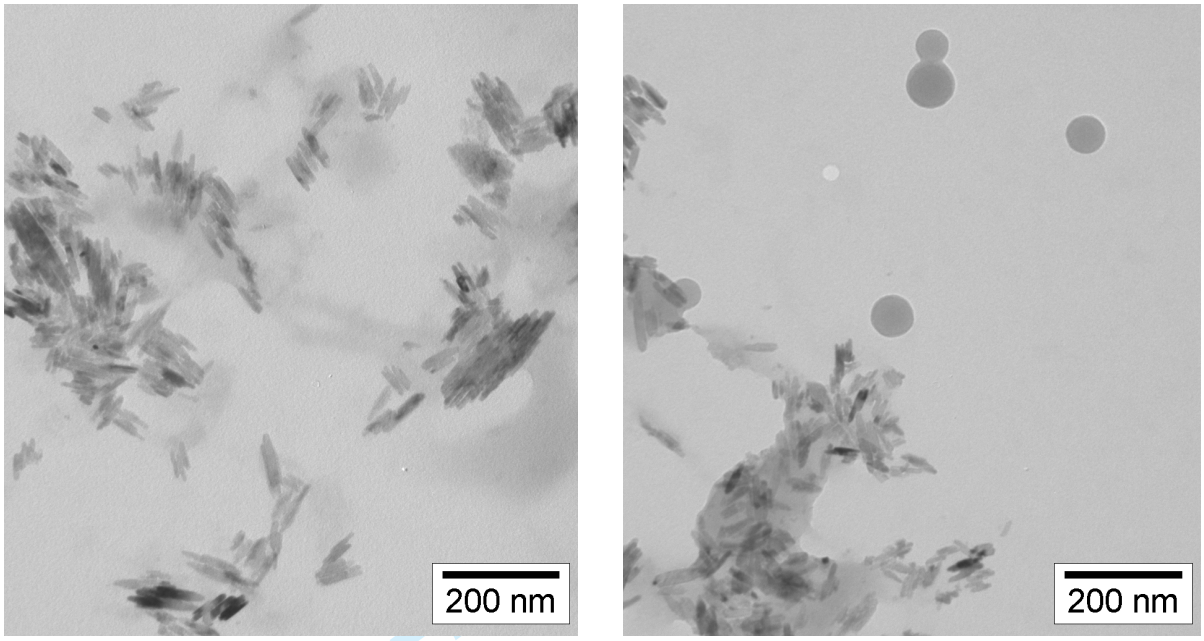

Figure 4. TEM pictures of EC10-containing a) miniemulsion and b) latex (EC content = 10 wt%, run 5). Note that for the miniemulsion, only ethyl cellulose is visible since the droplets disappear upon TEM observation.

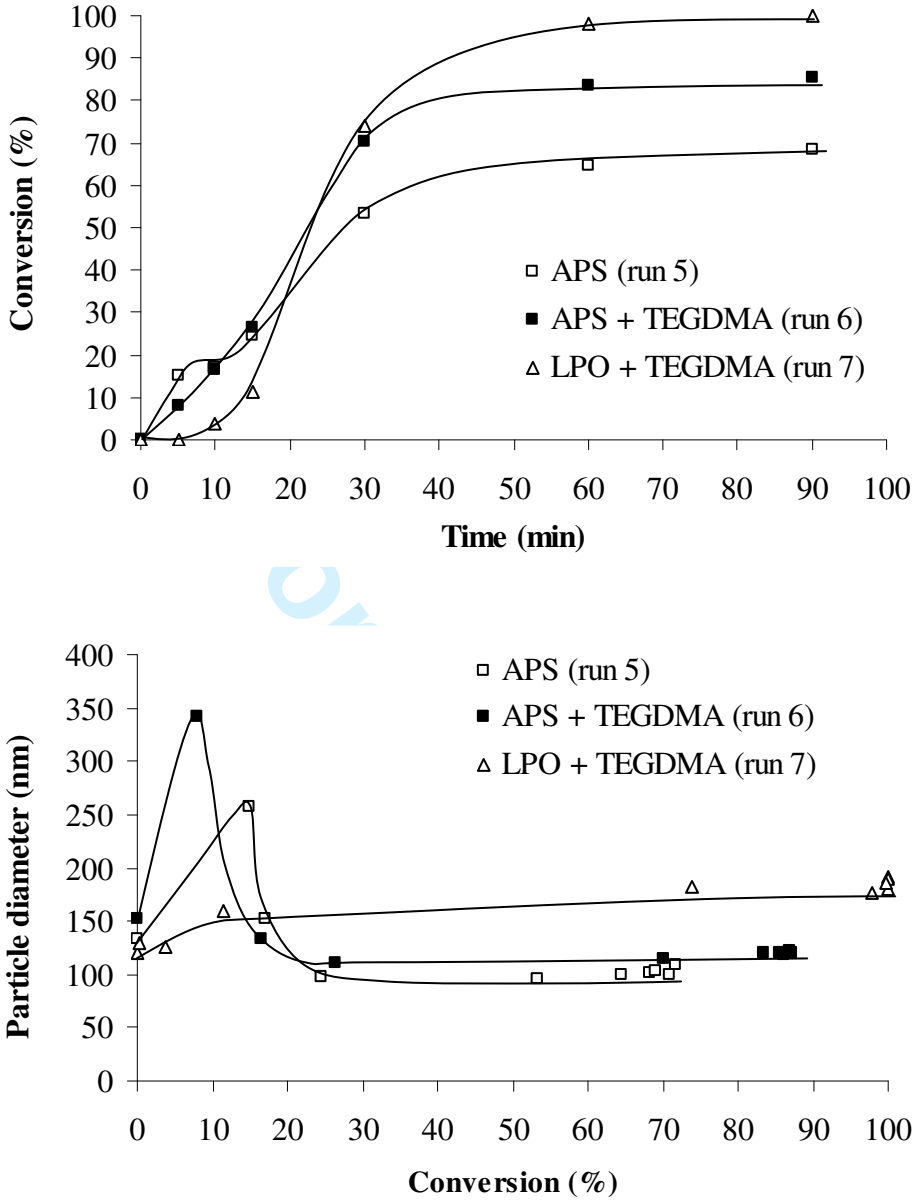

Figure 5. Effect of the addition of a cross-linker on the evolution of monomer conversion and particle size during miniemulsion polymerization of MMA and BA initiated by APS or LPO in the presence of 10 wt% of EC10. The lines are guides for the eye.

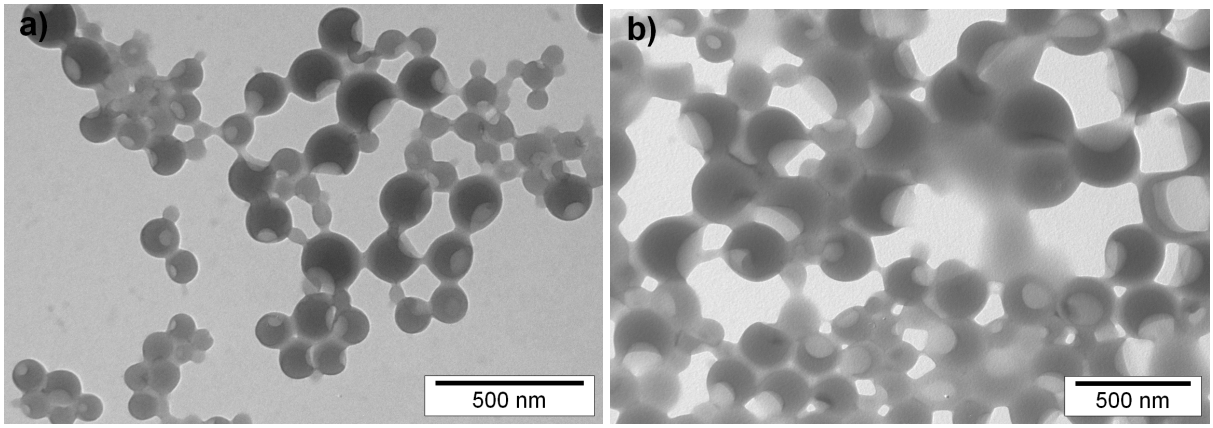

Figure 6. TEM pictures of LPO/TEGDMA-based systems a) without EC (run 8) and b) with 10 wt% of EC 10 (run 7).

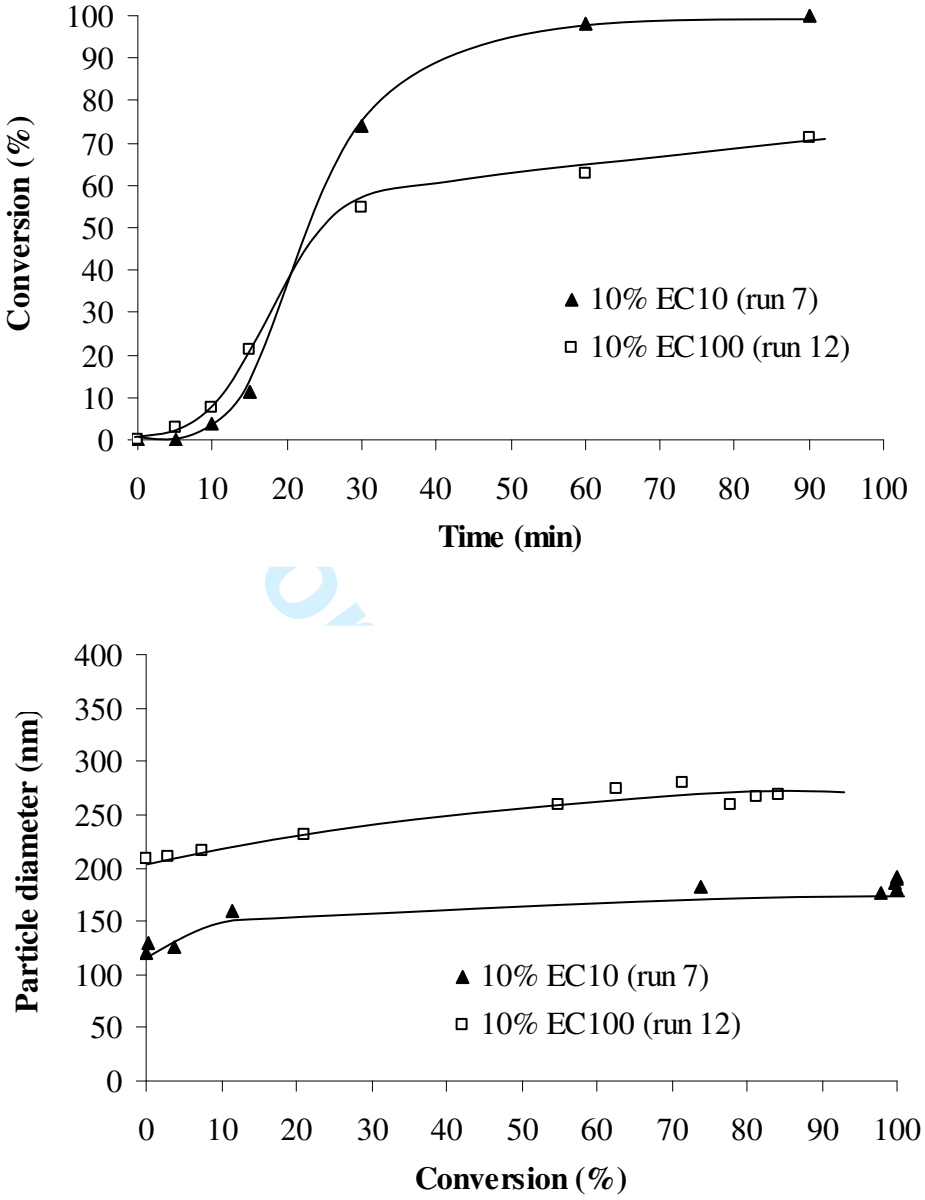

Figure 7. Evolution of monomer conversion and particle size during miniemulsion polymerizations of MMA and BA initiated by LPO in the presence of 4.7 wt% of TEGDMA and 10 wt% of EC10 (run 7) or EC100 (run 12). The lines are guides for the eye.

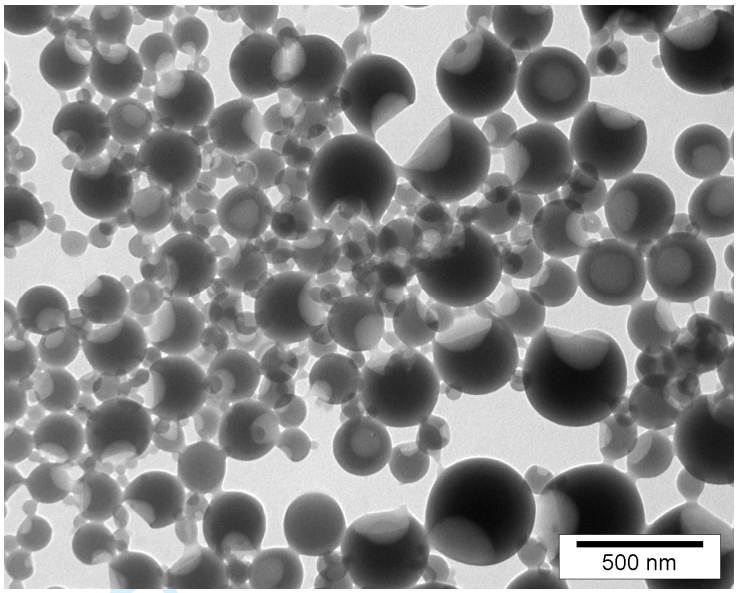

Figure 8. TEM image of EC100-based latex particles elaborated with LPO as initiator and TEGDMA as cross-linker (run 12).

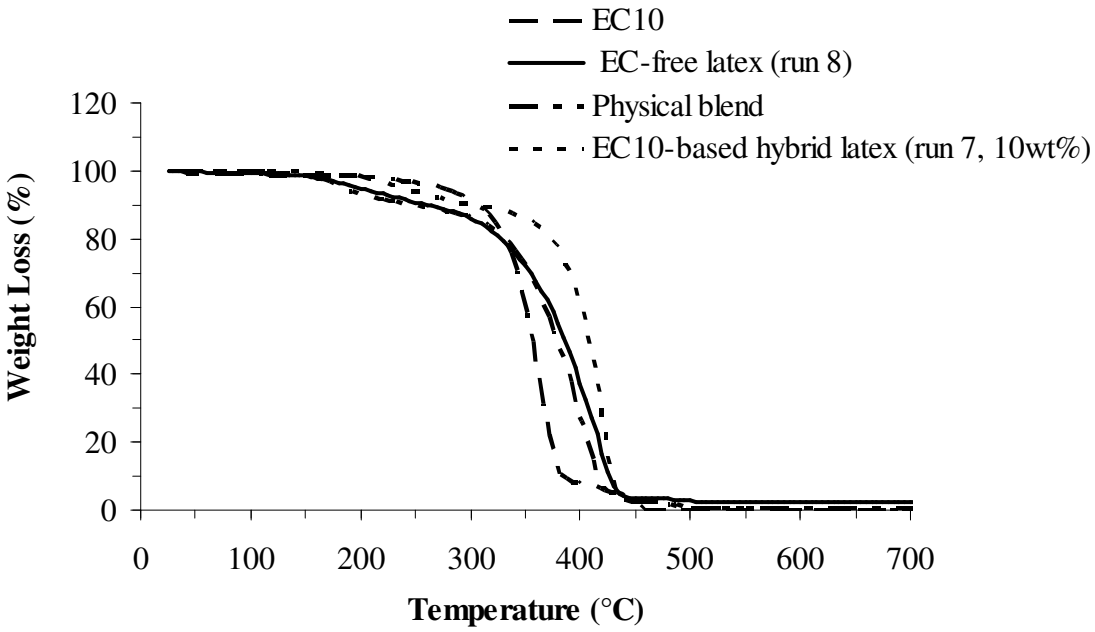

Figure 9. TGA curves of EC10 powder, an EC-free latex (run 8), a physical blend of EC10 powder (10 wt%) and an EC-free latex (run 8), and EC10-based hybrid latex (10 wt%, run 7).

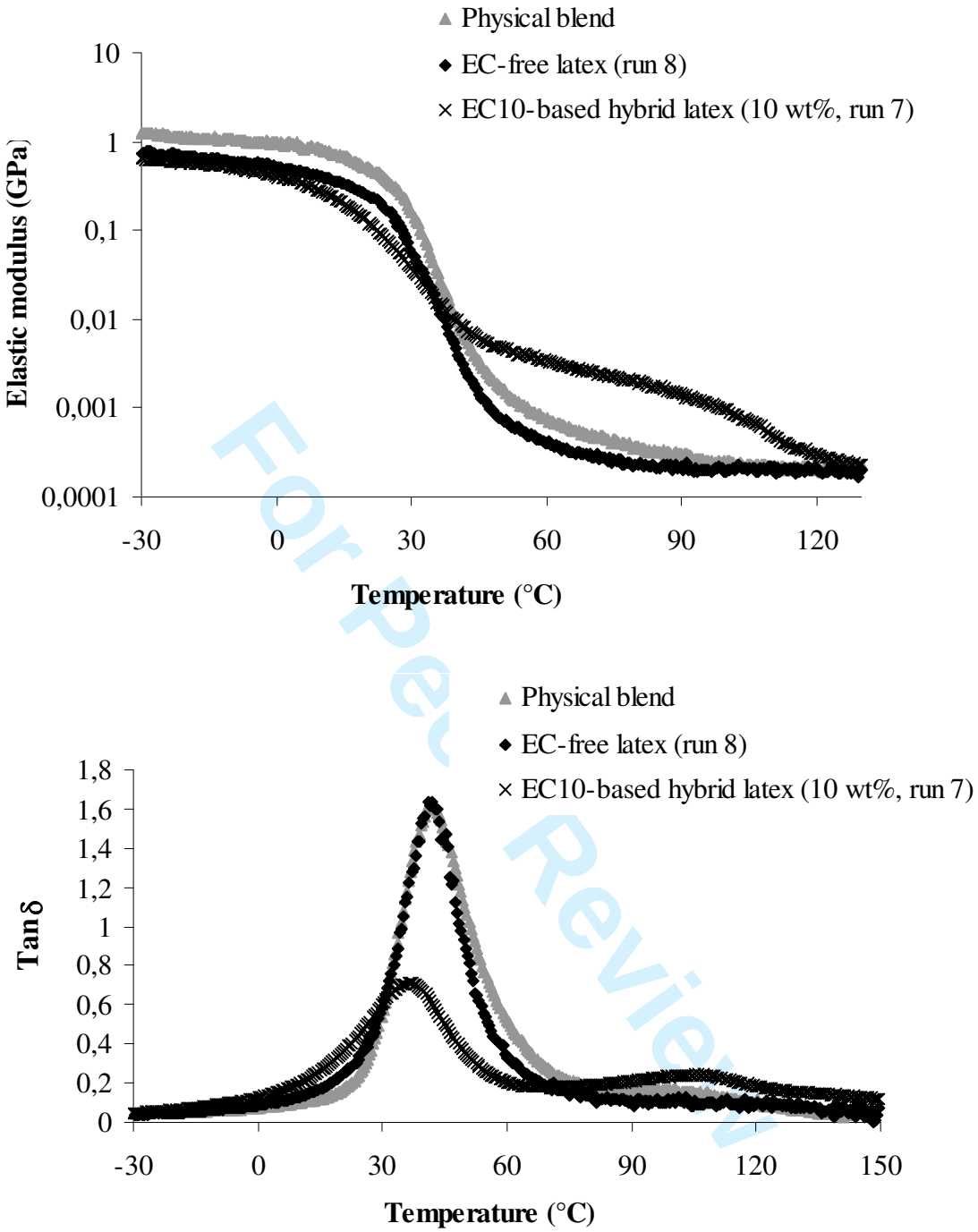

Figure 10. DMA curves of EC-free latex (run 8), of physical blend of latex and EC10 powder (10 wt%) and of EC10-based hybrid latex (10 wt%, run 7).

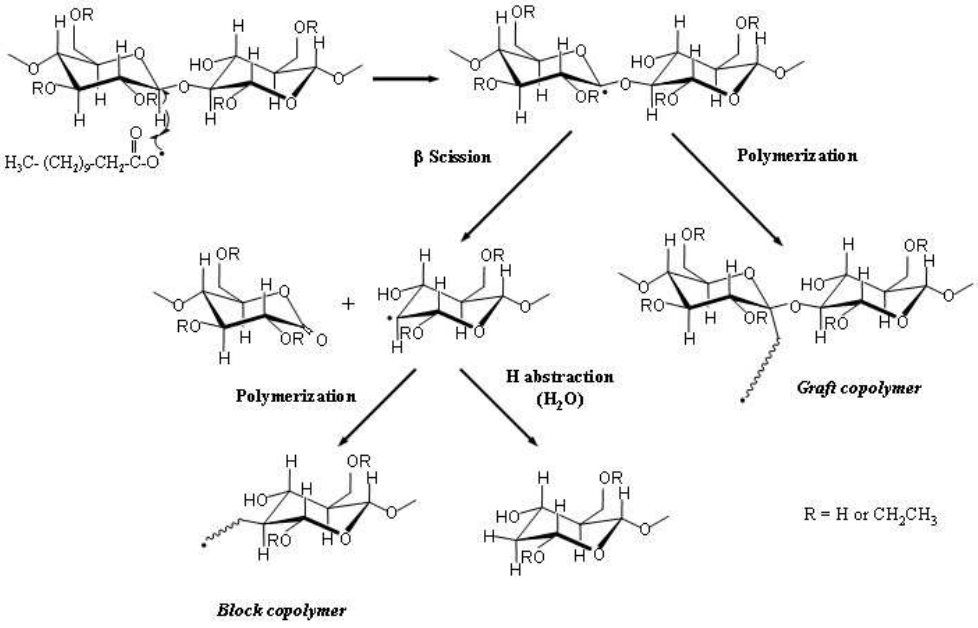

Mechanism for free-radical grafting and degradation of EC, adapted from the one proposed in reference 20.
189x129mm (96 x 96 DPI)

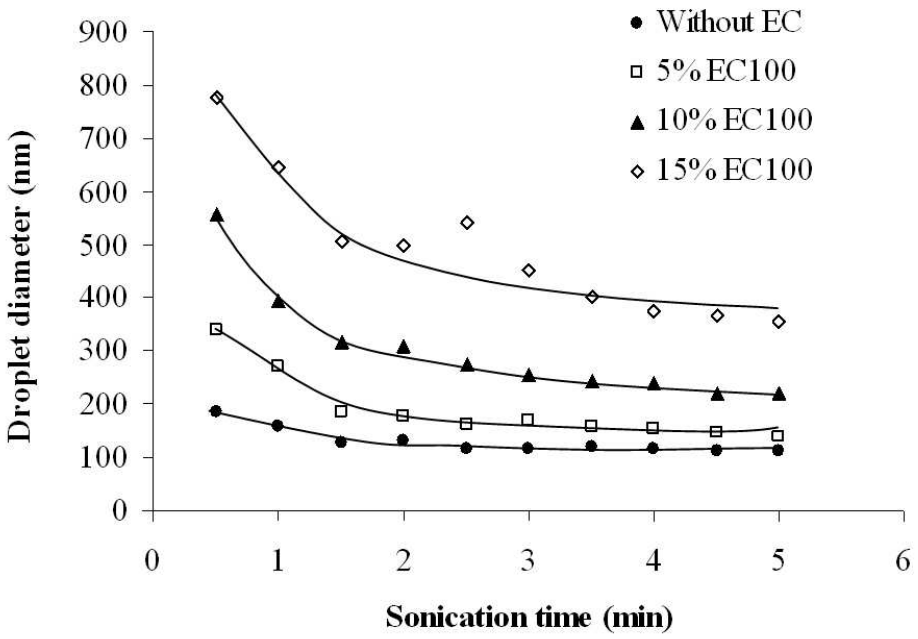

Droplet diameter vs sonication time for EC100-containing acrylic miniemulsions. The lines are guides for the eye. See Table 2 for experimental details.
254x169mm (96 x 96 DPI)

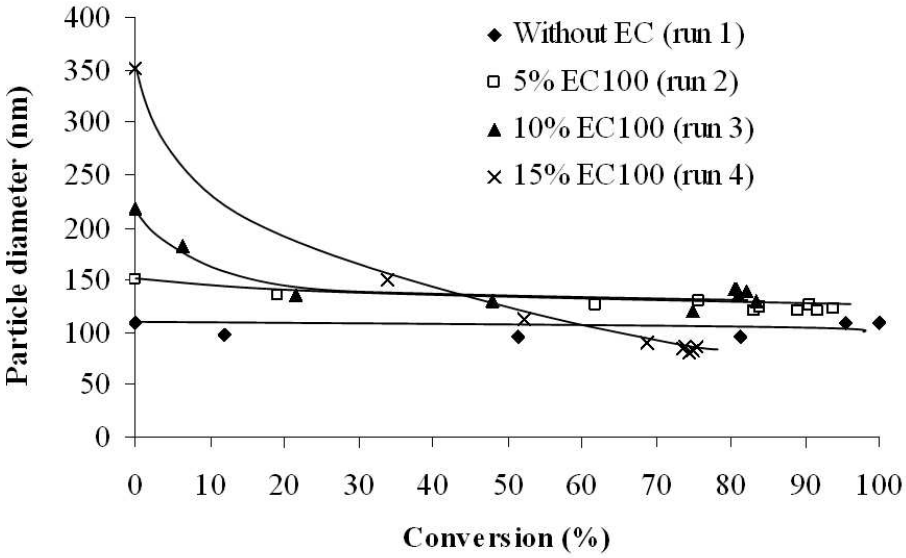

Evolution of particle size vs conversion during miniemulsion polymerization of MMA and BA in the presence of increasing EC100 contents. The lines are guides for the eye.
254x160mm (96 x 96 DPI)

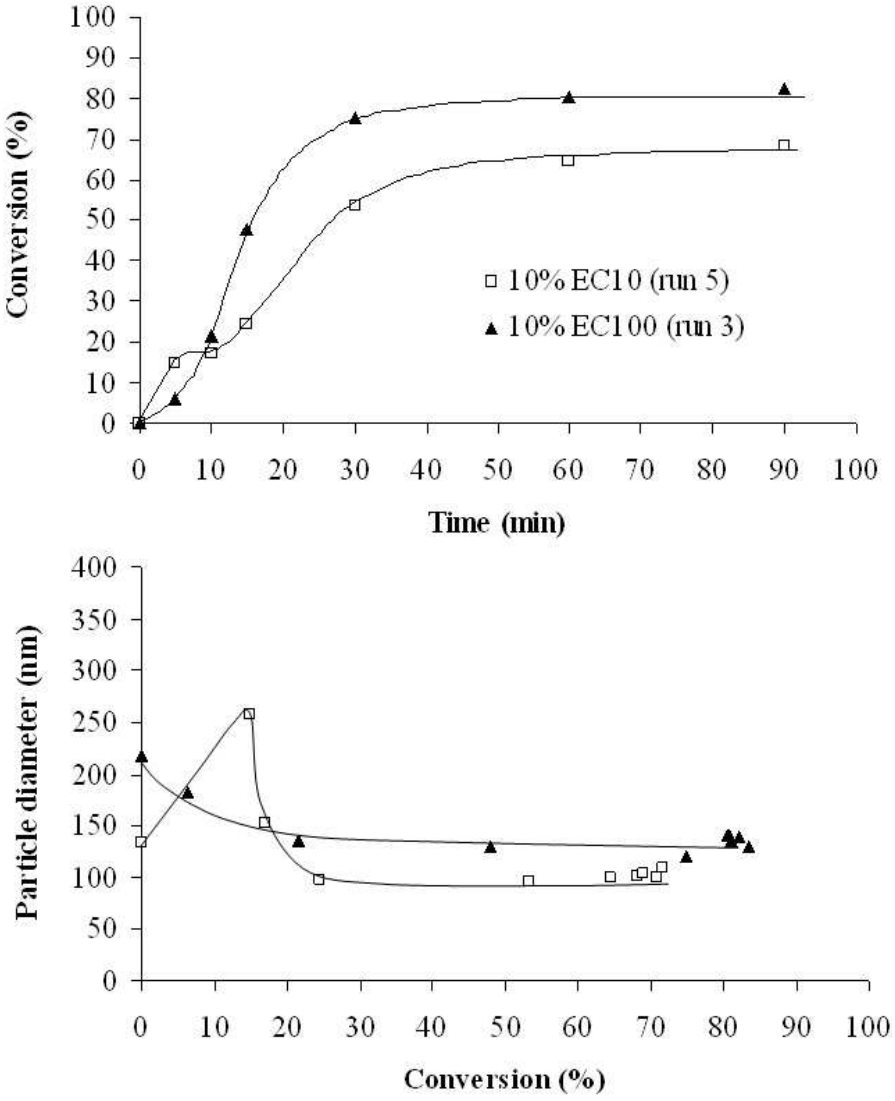

Evolution of monomer conversion and particle size during miniemulsion polymerization of MMA and BA in the presence of 10 wt% of EC10 (run 5) or EC100 (run 3). The lines are guides for the eye.
190x219mm (96 x 96 DPI)

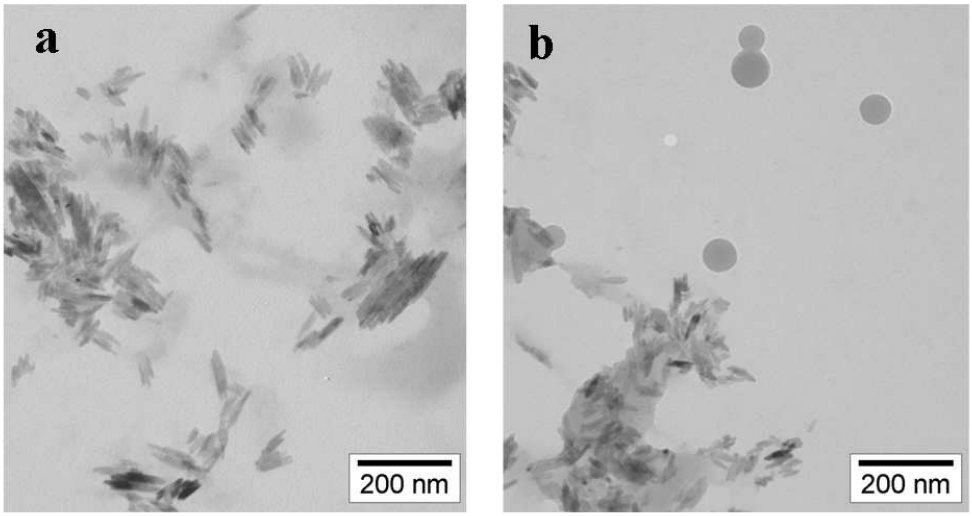

TEM pictures of EC10-containing a) miniemulsion and b) latex (EC content = 10 wt%, run 5). Note that for the miniemulsion, only ethyl cellulose is visible since the droplets disappear upon TEM observation.
254x139mm (96 x 96 DPI)

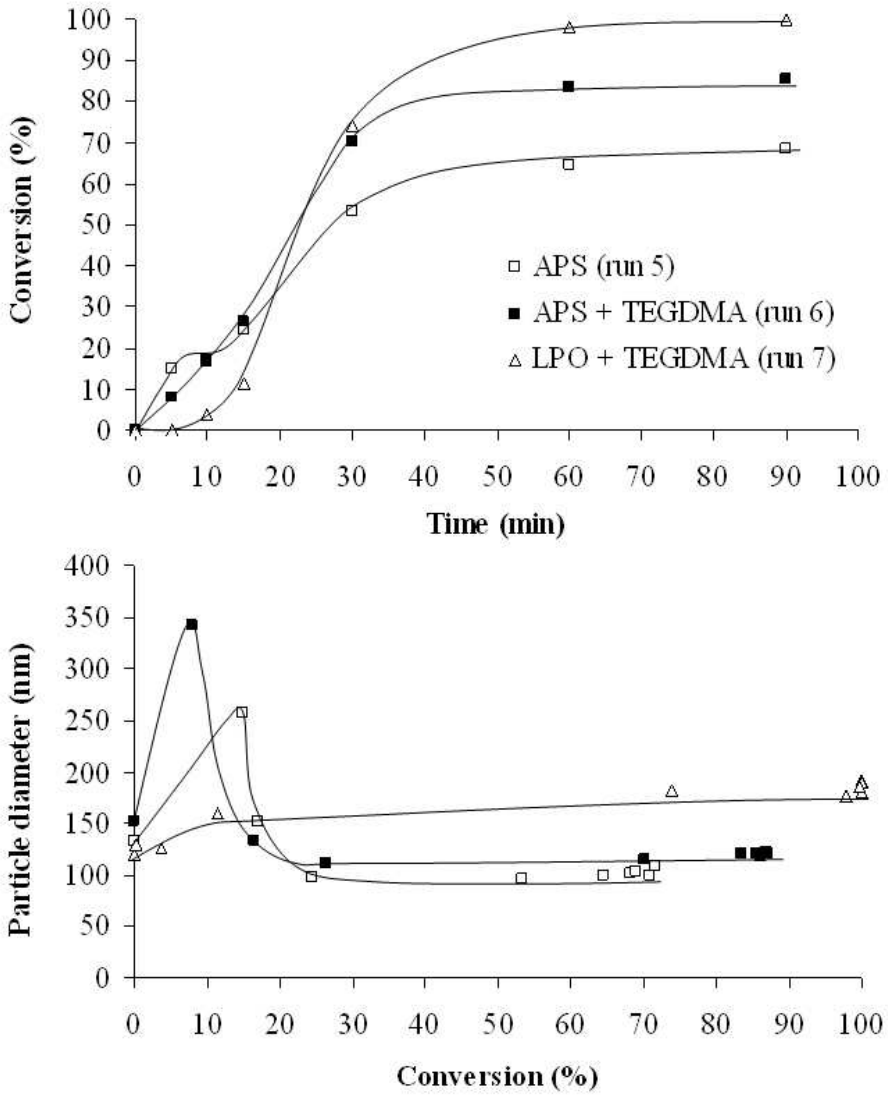

Effect of the addition of a cross-linker on the evolution of monomer conversion and particle size during miniemulsion polymerization of MMA and BA initiated by APS or LPO in the presence of 10 wt% of EC10. The lines are guides for the eye.
190x219mm (96 x 96 DPI)

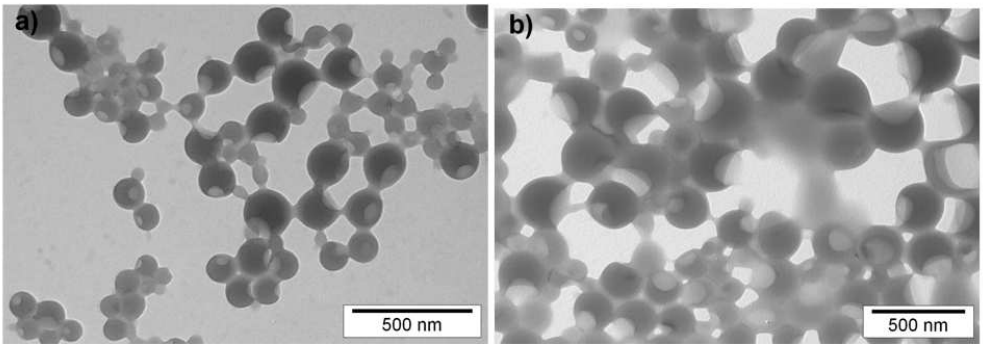

TEM pictures of LPO/TEGDMA-based systems a) without EC (run 8) and b) with 10 wt% of EC 10 (run 7).
254x100mm (96 x 96 DPI)

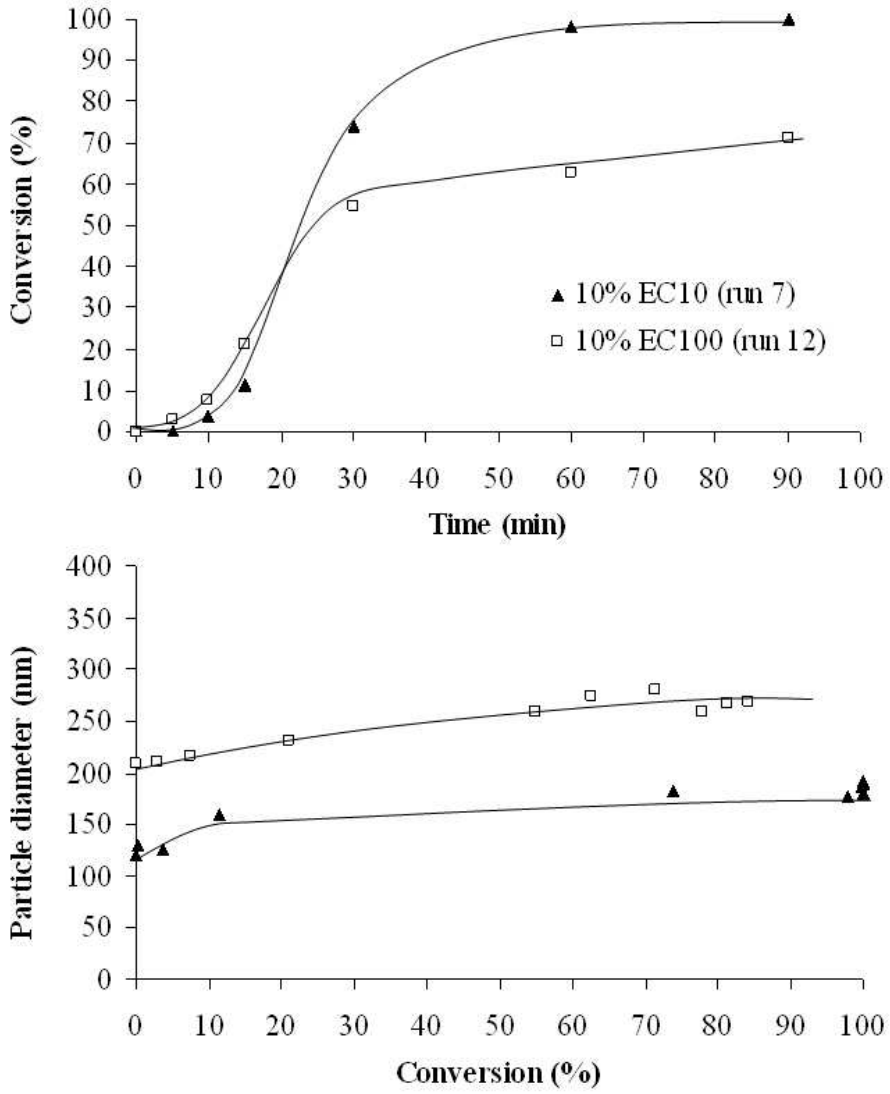

Evolution of monomer conversion and particle size during miniemulsion polymerizations of MMA and BA initiated by LPO in the presence of 4.7 wt% of TEGDMA and 10 wt% of EC10 (run 7) or EC100 (run 12). The lines are guides for the eye.
190x219mm (96 x 96 DPI)

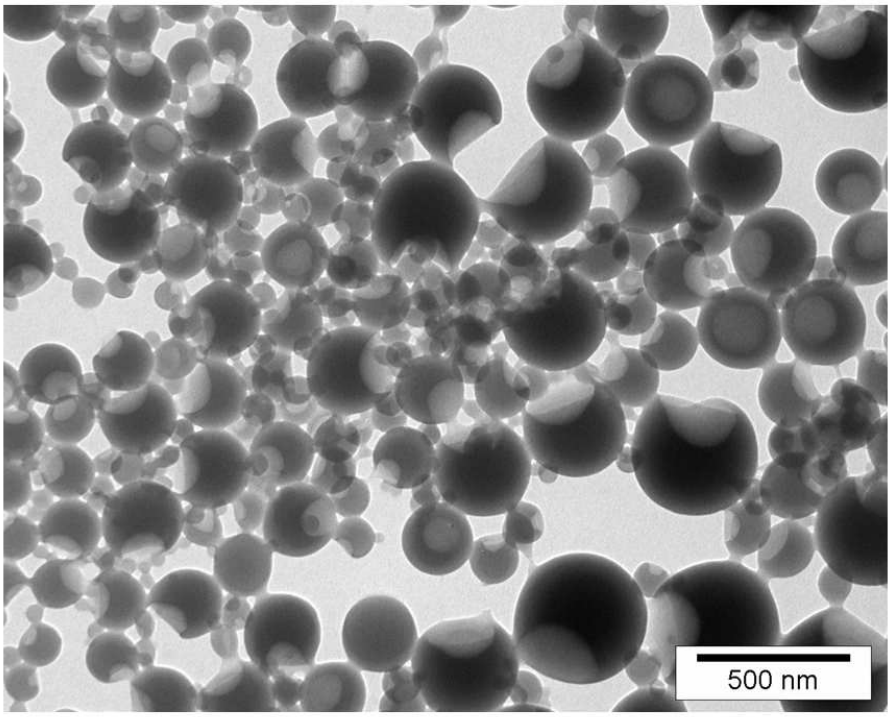

TEM image of EC100-based latex particles elaborated with LPO as initiator and TEGDMA as cross-linker (run 12).
254x190mm (96 x 96 DPI)

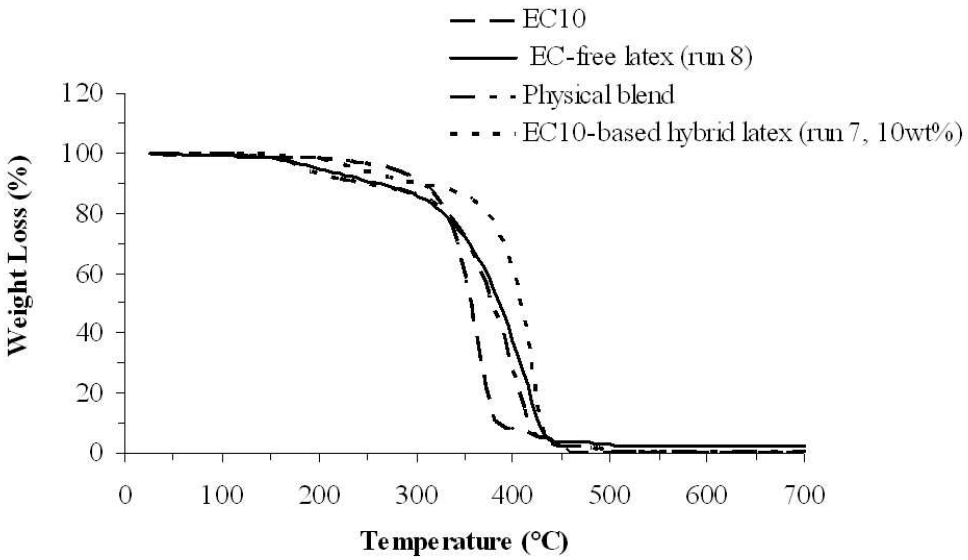

TGA curves of EC10 powder, an EC-free latex (run 8), a physical blend of EC10 powder (10 wt%) and an EC-free latex (run 8), and EC10-based hybrid latex (10 wt%, run 7).

254x150mm (96 x 96 DPI)

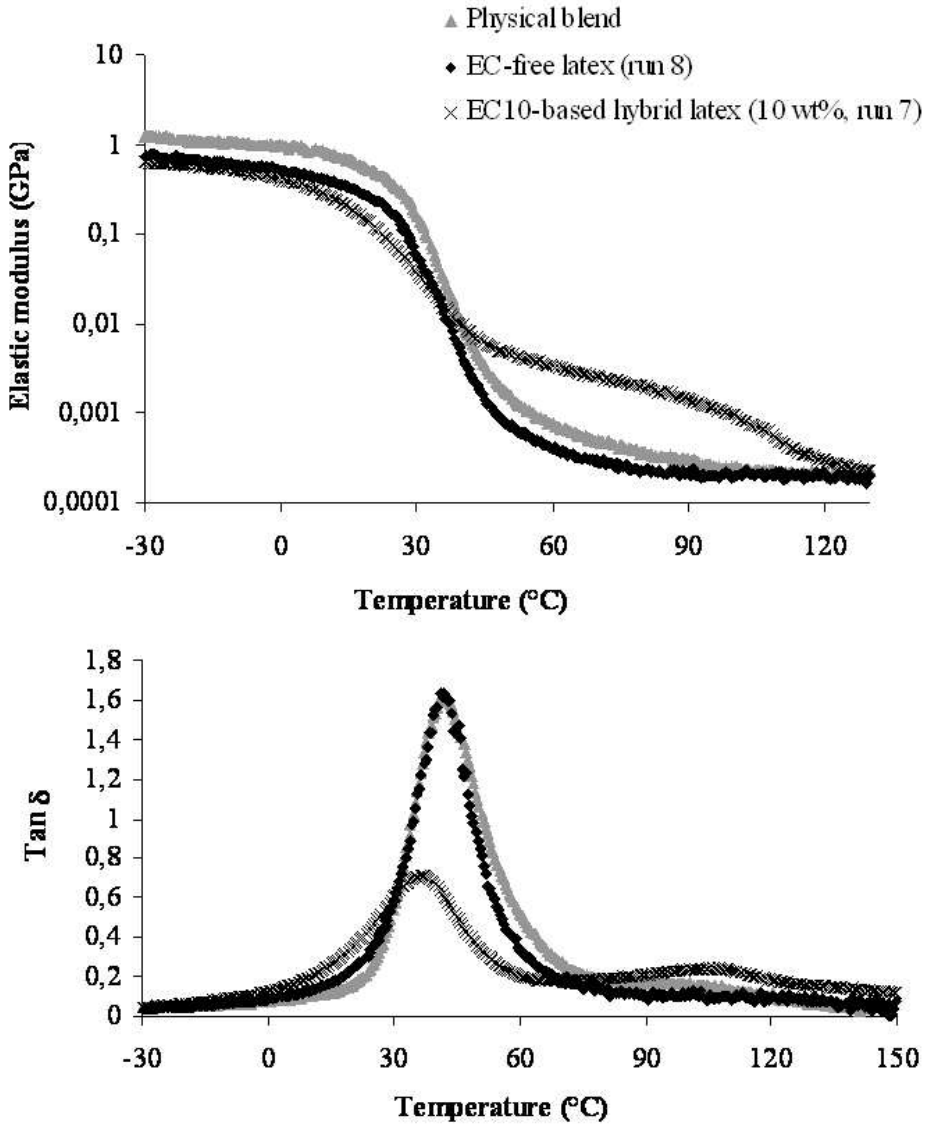

DMA curves of EC-free latex (run 8), of physical blend of latex and EC10 powder (10 wt%) and of EC10-based hybrid latex (10 wt%, run 7).
190x219mm (96 x 96 DPI)